

# Dyes Adsorption from Contaminated Aqueous Solution Using SiO<sub>2</sub> Nanoparticles Prepared from Extracted Tree Leaves

Wisam Adnan Hameed<sup>1</sup>, Mohammed Nsaif Abbas<sup>2\*</sup>

<sup>1</sup> Environmental Engineering Department, College of Engineering, Mustansiriyah University, Baghdad, Iraq

<sup>2</sup> Materials Engineering Department, College of Engineering, Mustansiriyah University, Baghdad, Iraq

\* Corresponding author's e-mail: mohammed.nsaif.abbas@uomustansiriyah.edu.iq

## ABSTRACT

The present study focused on the synthesis of silicon dioxide nanoparticles (SiO<sub>2</sub>) using a green method, incorporating buckthorn leaves extract and potassium metasilicate (K<sub>2</sub>SiO<sub>3</sub>) as the precursor. A comprehensive characterization of the prepared nanoparticles was performed using X-ray diffraction (XRD), fourier-transform infrared spectroscopy (FTIR), field emission scanning electron microscopy (FESEM), Brunauer-Emmett-Teller (BET) analysis, and dynamic light scattering (DLS). The results confirmed the purity of the SiO<sub>2</sub> nanoparticles and exhibited a range of diverse functional groups on their surface. Furthermore, the average size and surface area of the nanoparticles were determined to be 35.8 nm and 246 m<sup>2</sup>·g<sup>-1</sup>, respectively. These well-characterized SiO<sub>2</sub> nanoparticles were employed as an effective adsorbent for the removal of bromophenol blue dye from aqueous solutions in a batch mode adsorption unit, under varying operating conditions. The factors considered for evaluating the efficiency of SiO<sub>2</sub> nanoparticles as an adsorption media included pH, contact time, agitation speed, dye concentration, temperature, and the quantity of nanomaterial utilized. Experimental findings demonstrated a remarkable removal efficiency of 96% for bromophenol blue dye at an initial concentration of 100 ppm in the contaminated solution. Interestingly, the percentage removal exhibited an inverse relationship with dye concentration and temperature, while being directly proportional to other factors. Overall, the green-synthesized silicon dioxide nanoparticles proved to be a promising adsorbent for the effective removal of bromophenol blue dye from aqueous environments. The findings highlight the potential application of these nanoparticles in wastewater treatment and pollution mitigation, offering a sustainable and eco-friendly solution for environmental challenges.

**Keywords:** bromophenol blue dye, buckthorn leaves, extract, green method, silicon dioxide nanoparticles.

## INTRODUCTION

Water constitutes the fundamental essence of existence, serving as a cornerstone of life. However, when contaminated by pollutants, it ceases to be a source of sustenance, instead transforming into a perilous hazard to human well-being. Consequently, the oversight of potable water purity and safety surpasses that of food, given its ubiquitous consumption on a daily basis (Khaleel et al., 2022). The issue of water contamination stands as a primary concern for researchers and experts in the pollution domain. Multiple origins contribute to water pollution, notably including residues from chemical plants, mining activities, petroleum extraction, refinery operations, diverse

chemical compounds, heavy metal residues, dye residues, detergent residues, pesticide runoff, fertilizer runoff, agricultural by-products, soil leachate, as well as assorted organic and inorganic waste materials (Abd Al-Latif et al., 2023). Dyes represent pigmented compounds capable of adhering to substrates intended for coloring, imparting vivid hues that resist fading due to washing, light exposure, oxidation, acidic or alkaline conditions. Annually, a vast array of dyes is manufactured in substantial volumes, exceeding 100,000 varieties, each distinguished by its unique composition and constituents (Alwan et al. 2021). These substances find application across diverse sectors including dyeing, ink production, metal coating, tinting glass and ceramics, cosmetics

formulation, textile dyeing, food coloring, paper manufacturing, leather treatment, plastic production, pharmaceuticals, and chemical industries. Additionally, they serve as additives in oil refinement, photographic processing, and various other applications (Abbas and Alalwan, 2019). Due to its diversity, the increasing need for it, and its multiple uses in all industrial and agricultural fields, dyes have become one of the most important organic materials polluting water sources (Hanafi and Sapawe, 2020). Dyes have the potential to contaminate water through three primary pathways: firstly, through the raw materials utilized in their production, as these materials are derived from a variety of compounds with uncertain environmental characteristics, and the remnants of these substances frequently infiltrate water sources. Secondly, large volumes of wastewater are generated during the manufacturing process, with effluents from washing steps often containing (30–70%) of the permanent dyes, not to mention the volume of water left over from them (Williams et al., 2022). As for the last pathway, it is the industrial wastewater that contains high concentrations thereof, where approximately (10–15%) of the dyes used are dissipated. On the other hand, dyes are one of the common types of water pollutants due to their high-water solubility. Most synthetic dyes are highly toxic to humans and aquatic beings, and have acute as well as chronic effects (Kolya and Kang, 2024). For example, reactive dyes are notorious for causing health issues such as dermatitis, occupational asthma, rhinitis, and other allergic reactions for the workers involved in the manufacturing of these dyes. Dyes exhibit mutagenic and carcinogenic properties, resulting in chronic health effects including kidney, urinary bladder, and liver cancer among dye industry workers. An example is erythrosine, a xanthene dye known to be carcinogenic, neurotoxic, and capable of causing DNA damage in both humans and animals (Srivatsav et al., 2020). Therefore, the water contaminated with dyes needs rapid and efficient treatment to remove these hazardous chemicals to comply with the authorized limits so that they can be discharged into public sewage networks or into surface and ground waters (Abbas et al., 2019a). All of the mentioned effects are for dyes with known effect. As for the most dangerous type, they are the types of unknown effect on humans and animals, including dyes for biological activities (Ibrahim et al.,

2020a), medical studies, and scientific research, which are used to color tissue sections (Ibrahim et al., 2020b). So far, a number of these dyes have an unknown effect, which requires identifying, removing and disposing of their traces. It represents an important goal to preserve the purity of water sources and prevent potential environmental pollution resulting from their discharge to waterways and the environment (Alhamd et al., 2024). One of the most important types of these dyes is bromophenol blue, which a synthetic-colored dye is belonging to the thiazine family, derived from phenols (Hassen et al., 2022). It is odorless, color-changing according to pH, with a chemical formula ( $C_{19}H_{10}Br_4O_5S$ ), and soluble in water, benzene, acetic acid, sodium hydroxide, and alcohol (methyl and ethyl). This dye appears in the basic state in a bright blue-violet color, while in the acidic state it appears in a yellow color (NCBI 2023). This dye has many industrial, laboratory indicator and biological stain uses. Due to its unique properties, it is widely used as a pH indicator in laboratories, with this application being one of its most important uses. The dye is added to the solutions to monitor their color change with the change in pH, which makes it easier to measure the acidity or basicity values of the solutions (Aljubiri et al., 2023). In addition, it has many other important uses in chemistry sciences, molecular biology techniques, and numerous other fields. Through which the migration pathway can be determined in electrolysis in electrophoresis generation techniques to separate DNA or proteins and quantify them (NCBI 2023). This dye is also used in some cases in tissue and organ transplantation to determine the success of tissue transplantation and to ascertain whether it has been successfully accepted by the host body. On a related level, bromophenol blue dye is used to stain active and persistent genes in the genetic stream, as well as to examine gels and determine gel staining and loading control in genetics. Furthermore, it is used in testing the chemical composition of unknown aqueous solutions (Batubara et al., 2023). Scientists and researchers continue to pursue research and development to enhance its use and explore new applications for this important and beneficial dye in a wide range of scientific and industrial fields, making it a valuable and effective tool in modern science and research (Alshoaibi and Islam, 2021). Generally, while there is a lack of specific studies on

the toxicity of bromophenol blue, it is generally regarded as having low toxicity. Nevertheless, numerous adverse effects related to its toxic potential have been documented, emphasizing the need for careful handling and adherence to safety protocols. Inhalation of airborne bromophenol blue particles can lead to respiratory irritation (Abd Ali et al., 2024). Direct contact with the skin or eyes may result in irritation, and prolonged exposure could lead to congestion. Moreover, ingestion of substantial quantities of bromophenol blue may provoke irritation in the stomach or intestines, although the precise amount remains unspecified (NCBI 2023). Numerous techniques are employed to eliminate dyes or minimize their concentration to the lowest achievable level. These methods encompass chemical sorption, coagulation-flocculation, ozonation, advanced oxidation processes, biological treatments, extraction, reverse osmosis, ion exchange, ultrafiltration, nano-membrane filtration, adsorption, and various others. Among these approaches, the adsorption method emerges as a particularly promising technique for purging dyes from aqueous solutions (Abbas and Abbas, 2013a). This method is straightforward and cost-effective, necessitating neither extensive preparatory steps nor specialized equipment or substantial space. However, despite its simplicity, it has demonstrated remarkable efficacy in eliminating a wide array of contaminants (Alhamd et al., 2024), including heavy metals, organic compounds, inorganic toxins, and even dyes, from water, soil, and crude oil (Ali et al., 2021). One of the oldest and most important materials used as efficient and effective adsorption media is activated carbon due to its high surface area as well as the ability to deal with various types of pollutants and remove them from water (Maddodi et al., 2020). However, the high cost of preparing this material and its consumption during each reactivation process made it an obstacle to the progress of this treatment method (Rajaa et al. 2023). Agricultural and industrial wastes have attracted the attention of researchers and specialists in the field of pollution treatment for the advantages they possess as treatment media (Abbas and Abbas, 2013b). They are available materials that are non-valuable and must be disposed of, in addition to having effective aggregates and a suitable surface area that made them a successful alternative to activated carbon, as well as being materials with appropriate efficiency and good

effectiveness in treating pollutants (Abbas et al., 2020). These materials include banana peels (Abdullah et al., 2023), orange peels (Hasan et al., 2021), rice husks (Alalwan et al., 2018), lemon peels (Al-Hermizy et al., 2022), watermelon rinds (Abbas and Nussrat, 2020), pomegranate peels (Tolkou et al., 2024), egg shells (Ali et al., 2020a), aluminum foil (Ghulam et al., 2020), algae (Abbas et al., 2019b), water hyacinth (Ali and Abbas, 2020), waste tea leaves (Al-Ali et al., 2023) and others (Abdulkareem et al., 2023). A wide range of contaminants can be remediated by agricultural and industrial wastes, such as phenols (Ho, 2022), inorganic toxic (Alalwan et al., 2020), heavy metals (Hashem et al., 2021), hardness (Ibrahim et al., 2021), etc. Although the accumulation of these residues laden with toxic pollutants after the end of the adsorption process generated an additional problem that required disposal, the concept of the zero-residue level opened new horizons for benefiting from these residues (Hamdi et al., 2024). Instead of the need to eliminate these materials, it was possible, via this concept, to convert them into useful materials in an economical, low-cost, and environmentally friendly way, such as benefiting from them before using as an adsorption media in converting them after completion of their use into a rodenticide (Abd ali et al., 2018) as a result of their effects, or as a kind of fertilizer (Abbas, 2015), a nanomaterial (Alminshid et al., 2021), a concrete additive (Abbas et al., 2022a), or a useful substance (Abbas et al., 2022b). The current study aimed to take advantage of buckthorn leaves (as one of the types of agricultural waste) in the preparation of nano-silicon dioxide ( $\text{SiO}_2$ ) and to test the prepared material as a media for adsorption of bromophenol blue dye at different operating factors to determine the optimal conditions for recovering this dye from aqueous solutions.

## METHODOLOGY

### Preparation of plant leaves

Fresh buckthorn leaves were collected from local garden trees in the city of Baquba – Diyala Governorate, for the period from 01/11/2023 to 01/12/2023, and their classification was verified in the herbarium of the Department of Biology, College of Education for Pure Sciences – Diyala University. The collected leaves were washed

with an excess of tap water and then with distilled water twice to remove all impurities and dust stuck and left to dry naturally by exposing them to the open air in a clean place away from direct sunlight for a period of 24 hours. After drying ended, the process of grinding and crushing the leaves was carried out using manually using mortar and pestle and then by household grinder (Ultra Grinder Machine Pulverizer, Fengclock, China). After that, a sample of 10 g was sifted in a sieve analysis device (Mechanical Metal Powder Vibrating Sieve Analysis Shaker-DY200, 1–8 layers, China) according to the method described by (Rajaa et al., 2023), to choose powder of homogeneous size, and keep each powder in a separate opaque glass vial according to the size of the sieve. Table 1 shows the sieve analysis of the buckthorn leaves powder used in this study.

### Preparation of the plant extract

To prepare the buckthorn leaf extract, the powder passed through a 0.25 mm sieve was used, as it is the largest quantity produced according to Table 1. Before beginning the extraction process, the selected powder (of 50 mesh size) was dried in an oven at a temperature of 50 °C for half an hour, after that it was mixed with deionized distilled water in a suitable conical flask with a ratio of 1:8 (W/V). The flask was covered totally with a layer of aluminum foil to avoid the effects of light or light reactions may occur and also to limit the potential algal growth in the presence of adequate lighting. The extraction process was carried out by heating the mixture using a magnetic stirrer (Vevor Magnetic Stirrer Hot Plate) for half an hour at 70 °C and appropriate shaking. The mixture then filtered using Whatman filter paper 41, and the remaining filtrate was left to cool and

subsequently stored in a refrigerator at a temperature of 4 °C until later use.

### Synthesis of silicon dioxide nanoparticles

Silicon dioxide nanoparticles were synthesized through a well-controlled procedure. Initially, at a magnetic stirrer, a solution of 1 N potassium metasilicate ( $K_2SiO_3$ ) was added gradually (drop by drop) to the prepared buckthorn liquid extract at a ratio of 1:5 (V/V), with continuous stirring at 55 °C and 10 for temperature and pH, respectively, under reflux conditions. The continuous mixing for a duration of 12 hours, resulted in the successful synthesis of silicon dioxide nanoparticles. To adjust the pH level, 0.1 N KOH was carefully used. Then, the resulting mixture was subjected to filtration using Whatman filter paper No. 41, and the obtained precipitate was carefully washed three times with double distilled water to ensure removal of any impurities. The residues were separated from the mixture by centrifugation at 8000 rpm for 30 minutes. Subsequently, the separated solid phase was subjected to high-temperature treatment at 700 °C for 180 minutes in a furnace to eliminate any contaminants and organic components surrounding the silicon dioxide nanoparticles. Finally, a white precipitate of pure silicon dioxide nanoparticles was obtained, which was packed with and stored in an amber glass vessel with a secure plastic lid to maintain its quality and facilitate further characterization studies.

### Characterization of the prepared silicon dioxide nanoparticles

To identify the characteristic properties of prepared silicon dioxide nanoparticles, several physical tests were conducted. These tests were

**Table 1.** Sieve Analysis of buckthorn leaves powder used in this study

No.	Sieve size, (mm)	Mesh	Weight, (g)	% wt
1	0.500	35	0.853	8.53
2	0.354	45	1.584	15.84
3	0.297	50	3.128	31.28
4	0.250	60	1.967	19.67
5	0.149	100	1.353	13.53
6	0.088	170	0.942	9.42
7	Pan	–	0.173	1.73
Σ	–	–	10 g	100%

X-ray diffraction (XRD) carried out by X-ray diffraction (XRD) machine Shimadzu-XRD-6100, fourier-transform infrared spectroscopy (FTIR) performed by (FTIR Shimadzu 8400s device) within the range between 4000–400  $\text{cm}^{-1}$ , field emission scanning electron microscopy (FE-SEM) conducted by (Inspect f 50 FEI) device with 25,000  $\times$  magnification, Brunauer–Emmett–Teller (BET) surface area achieved by (Quantachrome, Qsurf 9600 Thermo Finnegan Co., USA device), and dynamic light scattering (DLS) determined by heat flux differential scanning calorimetry (Shimadzu DSC-60).

#### Dynamic light scattering)

The analysis of particle size distribution was conducted using dynamic light scattering (DLS) technique. The findings of this study revealed that the average size of silicon dioxide nanoparticles synthesized through the green method using buckthorn leaves extract and potassium metasilicate ( $\text{K}_2\text{SiO}_3$ ) as a precursor was determined to be 35.8 nm, as depicted in Figure 1. The DLS analysis indicated that the particle size remained relatively consistent, indicating a stable synthesis process. The observed particle size distribution curve exhibited a sharp peak, indicating a high level of uniformity, homogeneity, and mono-dispersity among the synthesized nanoparticles, with minimal variation in size. This outcome can be attributed to the elevated temperature treatment of the precipitate during the preparation process,

resulting in the breakdown of larger structures into smaller particles. Additionally, the use of a concentrated extract (used without further dilution) and the availability of abundant raw materials from the potassium metasilicate ( $\text{K}_2\text{SiO}_3$ ) contributed to these favorable results. The duration and reflux conditions employed in the synthesis process played a crucial role in achieving this particular particle size distribution outcome.

#### X-Ray diffraction

The crystalline structure of the synthesized nanoparticles was investigated using X-ray diffraction analysis. The XRD analysis was conducted at room temperature, employing  $\text{CuK}\alpha$  (1.5406 Å) radiation and covering a  $2\theta$  range from 20 to 80°. Figure 2 illustrates the XRD patterns obtained for the  $\text{SiO}_2$  nanoparticles synthesized through the green method, utilizing buckthorn leaves extract and potassium metasilicate ( $\text{K}_2\text{SiO}_3$ ) as a precursor. The XRD diffractograms exhibited a broad intense peak centered between 19–22°, indicating the presence of an amorphous structure in the synthesized nanoparticles. Notably, no other diffraction peaks were observed, suggesting the absence of any additional crystalline phases in the nanoparticles.

The obtained peaks were found to be in agreement with the reference JCPDS file No. 89–0510 for  $\text{SiO}_2$ , further confirming the composition of the synthesized nanoparticles. It is worth mentioning that the absence of impurities peaks for  $\text{SiO}_2$

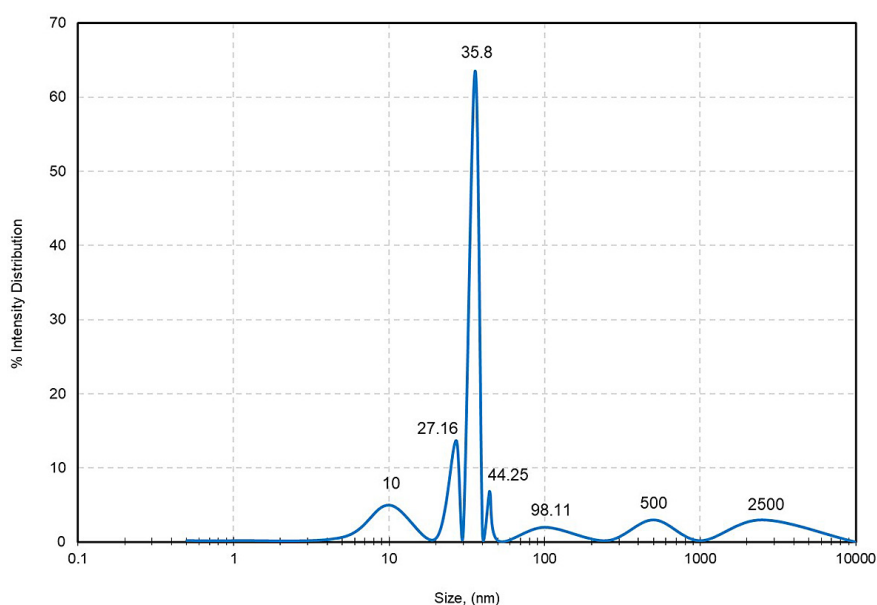
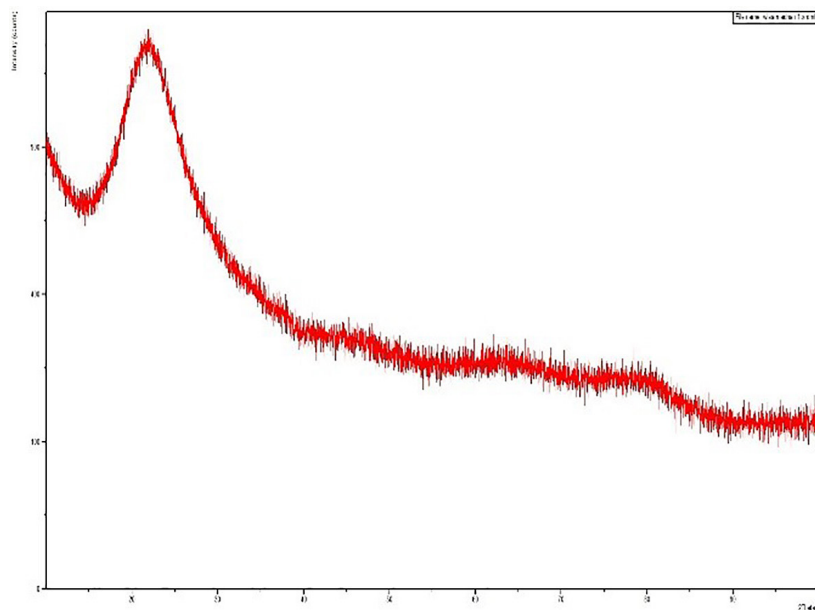


Figure 1. DLS analysis of silicon dioxide nanoparticles prepared



**Figure 2.** XRD of silicon dioxide nanoparticles prepared

indicates the purity of the synthesized nanoparticles. The amorphous nature of the nanoparticles can be attributed to the calcination process, which caused a transformation of the precursor’s crystalline structure into amorphous particles (Alalwan et. al., 2022a). This transformation is consistent with the well-known behavior of crystalline structures at temperatures around  $700^\circ\text{C}$ , where amorphous particles are typically formed. The XRD analysis provides valuable insights into the crystalline structure of the synthesized  $\text{SiO}_2$  nanoparticles, confirming their amorphous nature and purity. These findings support the successful synthesis of  $\text{SiO}_2$  nanoparticles

through the green method utilizing buckthorn leaves extract and potassium metasilicate as a precursor (Abbas and Abbas, 2013c).

*Fourier transform infrared spectroscopy (FT-IR)*

The FTIR spectra of the silicon dioxide nanoparticles synthesized using the green method are depicted in Figure 3. The spectrum reveals the presence of two outstanding peaks alongside several minor peaks. Specifically, the peaks observed at  $791.92\text{ cm}^{-1}$ ,  $806.44\text{ cm}^{-1}$ , and  $1091.67\text{ cm}^{-1}$  correspond to the symmetric and asymmetric stretching vibrations

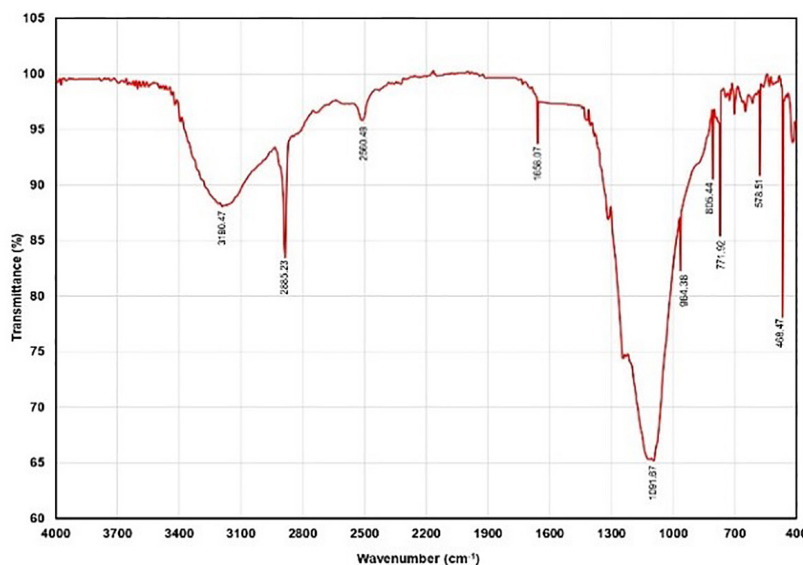


**Figure 3.** FTIR spectrum of silicon dioxide nanoparticles prepared

of Si-O-Si bonds. The bending vibration of siloxane (Si-O-Si) is represented by the bands at  $468.47\text{ cm}^{-1}$  and  $578.51\text{ cm}^{-1}$ . An absorption peak at  $964.38\text{ cm}^{-1}$  indicates the asymmetric stretching of Si-OH bonds. Furthermore, the absorption peak at  $1658.07\text{ cm}^{-1}$  is attributed to the bending vibration of water molecules adsorbed on the surface of the silicon dioxide nanoparticles. Although the intensity of this peak can be reduced by heating, it cannot be completely eliminated. The peaks observed at  $2560.49$  and  $2885.23\text{ cm}^{-1}$  represent the symmetric stretching vibrations of alkyl groups. Additionally, the absorption peak at  $3190.47\text{ cm}^{-1}$  corresponds to the asymmetric stretching vibrations of alkyl groups. These characteristic peaks strongly support the successful synthesis of a highly reactive surface in the silicon nanoparticles derived from buckthorn leaves extract and potassium metasilicate ( $\text{K}_2\text{SiO}_3$ ) as a precursor.

#### Field emission scanning electron microscopy

The surface morphology of the silicon dioxide nanoparticles was primarily determined by field emission scanning electron microscopy (FESEM) test, and the result is shown in Figure 4. It can be seen that the majority of the nanoparticles sample is on the nanoscale and possess asymmetric spherical shape with smooth surfaces. Also, it is clear that the green synthesized method produces poly-disperse nanoparticles with different particle sizes. This is related to the state of balance between nucleation and growth processes which results in non-isotropic growth of particles when misalignment. In narrow limit, there are a tendency for agglomeration between the prepared particles as clear from the FESEM test. The formation of tiny particles as a result of low preparation temperature where the nanoparticles produced at higher temperature  $> 70\text{ }^\circ\text{C}$  favored non-spherical morphology whilst spherical particles are obtained at lower temperature ( $< 60\text{ }^\circ\text{C}$ ). This may be due to the different growth rates of particles in different directions. Generally, the agglomeration process is a characteristic of the green synthesis method and is performed due to a consequence of the impact of interparticle forces on particle sizes lesser than  $1\text{ }\mu\text{m}$ . If the concentrations of raw materials are high (as in this study), this led to the high ionic strength of the solution that, in turn, increases nucleation and growth rates of particles. Double layer thickness is not considerable in solutions with high ionic strength and, therefore, the possibility of agglomeration enhances some primary particles

tending to aggregate and form large secondary particles. Under these conditions, primary nuclei form, grow very fast, agglomerate and make large nanoparticles (Alalwan et al., 2022b).

#### Specific surface area

The surface area ( $S_{\text{BET}}$ ) is an important parameter to evaluate the operational characteristics of catalysts, adsorbents and any other porous media. In this study, the surface area was meticulously determined for the silicon dioxide nanoparticles synthesized using the green method, employing buckthorn leaves extract and potassium metasilicate ( $\text{K}_2\text{SiO}_3$ ) as a precursor. The measurement process involved physical adsorption-desorption analysis of nitrogen gas at a constant temperature equivalent to the boiling point of liquid nitrogen ( $-77\text{ K}$ ). The resulting adsorption-desorption isotherm, depicted in Figure 5 exhibits a characteristic IV category curve, indicating the presence of mesoporous structures and slit-like pores. The adsorption process initially saturated the micropores of the material (at  $P/P^\circ = 0.34513$ ), followed by the filling of mesopores with multilayers of nitrogen gas. The specific surface area of the synthesized silicon dioxide nanoparticles was remarkably high, reaching an impressive value of  $246\text{ m}^2/\text{g}$ . Notably, this specific surface area surpassed those reported for ordinary silicon dioxide materials. For instance, regular spherical silicon dioxide particles with a diameter of  $0.5\text{ }\mu\text{m}$  (or  $200\text{ nm}$ ) exhibited a surface area of only  $14.29\text{ m}^2/\text{g}$ , measured using the Multi-Point Brunauer–Emmett–Teller (BET)

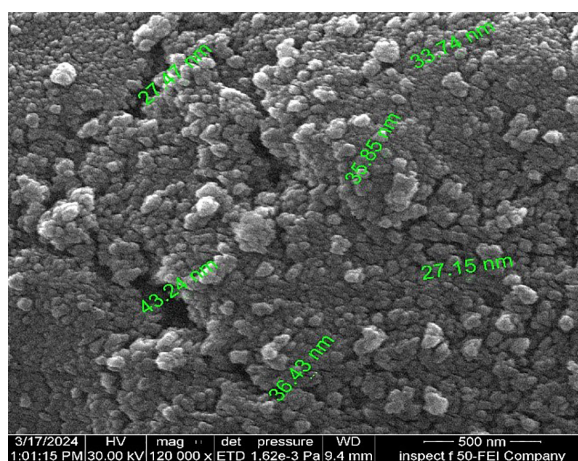


**Figure 4.** FESEM of the silicon dioxide nanoparticles prepared

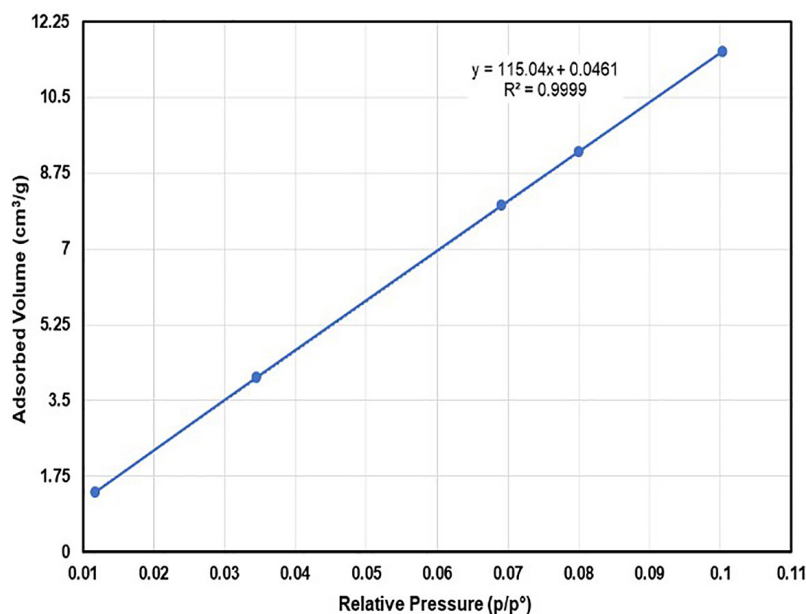


**Figure 5.** Adsorption-desorption isotherm for the silicon dioxide nanoparticles prepared

method. The elevated surface area of nanomaterials can be attributed to their significantly reduced particle size compared to conventional materials. The nanoscale size allows for a higher number of particles per unit volume, resulting in an increased active surface area available for interactions with other compounds and the surrounding environment. Moreover, the structural characteristics of nanoparticles, including their smaller and more branched particle morphology, further enhance the interfacial area between the particles and the surrounding medium. These additional surface sites play a crucial role in facilitating various surface phenomena, such as chemical reactions, physical interactions, material adsorption, and molecular exchanges. Furthermore, nanoparticles possess unique surface properties, such as thinness, smoothness, and subtle atomic-level structural deformations, which contribute to their enhanced surface activity.

### Stock solution of tested dye

The stock solution of bromophenol blue dye (CAS: 115-39-9) was prepared using reddish-violet powder procured from Wuhan Golden Wing Industry & Trade Co., LTD, Shanghai, China. To prepare the solution, exactly 500 mg of the dye was dissolved in one 0.5 liter of laboratory-prepared double distilled water using a water distillation unit (GFL-2012). This

meticulous procedure ensured that each cubic centimeter of the solution contained 1 mg of bromophenol blue dye, resulting in a concentration of 1,000 ppm. The use of high-quality double distilled water guaranteed the purity and accuracy of the solution, eliminating any potential interference from impurities.

### Calibration curve

The determination of the maximum wavelength ( $\lambda_{\max}$ ) of the bromophenol blue dye involved conducting a series of laboratory experiments with a fixed concentration of 10 ppm. The wavelength range explored ranged from 200 nm to 900 nm. These experiments were carried out using a precise spectrophotometer device, specifically the FTIR Shimadzu 8400 s. At each wavelength, the absorbance of the dye was measured and recorded. These absorbance values were then plotted using the same method described in (Ali et al., 2020b), resulting in Figure 6. From the plot, it was observed that the maximum absorbance value reached 0.999. This maximum absorbance occurred at a wavelength of 590 nm, which was determined to be the most optimal wavelength for this particular dye. The chosen wavelength of 590 nm was subsequently used to generate the calibration curve for bromophenol blue dye, as illustrated in Figure 7. This curve allows for accurate

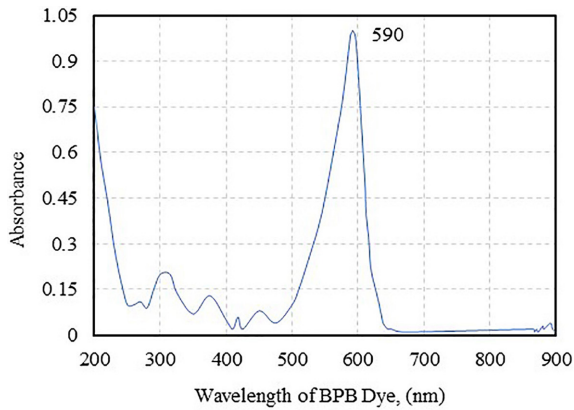


**Figure 6.** Absorbance due to wavelength changing of bromophenol blue dye

quantification of the dye's concentration in future experiments and analyses. By utilizing the wavelength of 590 nm, researchers can confidently assess the presence and concentration of bromophenol blue dye in various samples.

#### Adsorption unit used

The batch adsorption experiments of bromophenol blue dye using prepared silicon dioxide nanoparticles were conducted in a specialized adsorption unit. A specific concentration of bromophenol blue dye was prepared by diluting the required amount of the stock solution. The objective was to determine the optimal operating conditions that would yield maximum removal efficiency. Various design parameters, including pH, agitation speed, initial concentration, contact

time, temperature, and dose of silicon dioxide nanoparticles, were investigated. The pH of the solution was controlled using 0.1 N sodium hydroxide (NaOH) and 0.1 N hydrochloric acid (HCl) solutions. The range of parameters explored was as follows: pH (1–9), agitation speed (100–400 rpm), initial concentration (1–125 ppm), contact time (10–180 minutes), temperature (25–50 °C), and nanoparticle dose (0.01–0.11 g). Each experiment involved adding 100 ml of the bromophenol blue solution, with specific concentrations and pH values, to a sealed conical flask (150 ml Pyrex® Borosilicate glass with glass stopper). The flask was then placed in a water bath shaker, and the experiment commenced by setting the desired agitation speed. The experiment duration was determined by the predefined contact time. After completion, the solution was filtered using a vacuum filtration apparatus (JOANLAB VP-10L), and the silicon dioxide nanoparticles were separated. The remaining concentration of bromophenol blue dye in the treated solution was measured using spectrophotometry. The percentage removal of dye and the adsorption capacity of the silicon dioxide nanoparticles were calculated using Equations 1 and 2, respectively.

$$\%E = \left(1 - \frac{C_f}{C_o}\right) \times 100 \quad (1)$$

$$q = \frac{V}{1000} \frac{(C_o - C_f)}{m} \quad (2)$$

where: %*R* – represents the removal efficiency of bromophenol blue dye, calculated as the percentage of dye removed from the initial

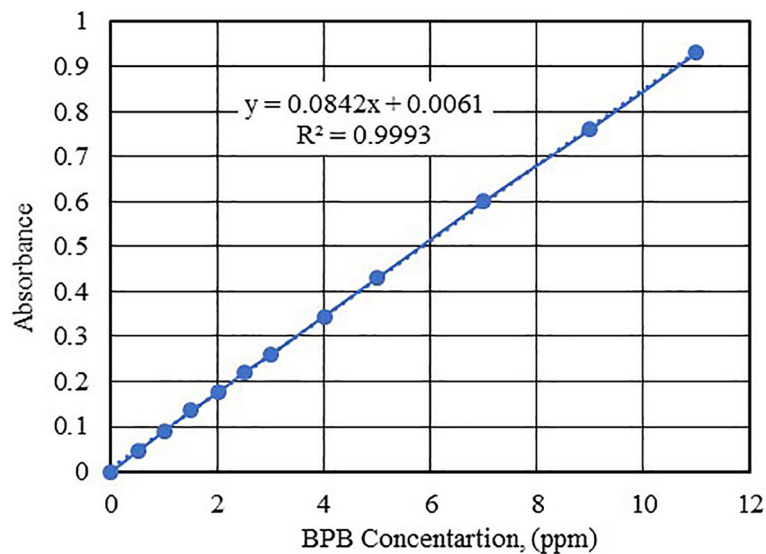


**Figure 7.** Calibration curve of bromophenol blue dye using UV-spectrophotometer

concentration  $C_o$  to the final concentration  $C_f$  – measured by (ppm),  $q$  – represents the adsorption capacity of silicon dioxide for bromophenol blue dye, expressed in mg/g. It quantifies the amount of dye adsorbed by a given mass of silicon dioxide,  $V$  – represents the volume of the solution used in the adsorption experiment, measured by ml, and  $m$ : represents the amount of silicon dioxide used in the adsorption process.

Overall, this experimental setup allowed for the evaluation of the adsorption performance of silicon dioxide nanoparticles in removing bromophenol blue dye, providing valuable insights into the effectiveness of various operational parameters. Equations 1 and 2 allow for the quantitative assessment of the adsorption performance, providing valuable information on the effectiveness of silicon dioxide nanoparticles in removing dye from solution.

## RESULTS AND DISCUSSION

### Behavior of acidic function

The pH of the dye solution plays a crucial role in the adsorption process as it influences both the chemical composition of the dye molecules and the surface properties of the adsorbent. In order to understand the impact of pH on the adsorption process using silica dioxide nanoparticles, the pH was varied within a range of 1 to 9 while keeping other variables constant at their optimum values.

The relationship between the removal efficiency of bromophenol blue dye from aqueous solutions and the pH was investigated, as shown in Figure 8. It is evident from the figure that there is an inverse correlation between the removal efficiency and pH, with higher removal efficiency achieved at lower pH values and vice versa. The percentage removal of bromophenol blue dye decreased from 90.732% to 6.179% as the pH increased from 1 to 9, respectively. This behavior can be attributed to the nature of bromophenol blue dye, which is classified as an acidic (anionic) dye and dissociates into negatively charged ions when dissolved in water. At low acidic pH values, the surface of silica dioxide nanoparticles becomes positively charged due to an increase in the concentration of hydrogen ions ( $H^+$ ) in the solution. This results in increased attraction forces between the positively charged adsorbent surface and the negatively charged bromophenol blue dye molecules, leading to enhance the removal efficiency and adsorption capacity, consequently, the amount of dye adsorbed is increased (Mohammed Ali et al., 2022). The decreasing in the removal efficiency was continued dramatically with increasing pH beyond the neutral level, i.e., when the pH value exceeds 6, the removal efficiency of bromophenol blue dye is significantly lower, reaching approximately 6% at pH of 9. This can be attributed to the huge increasing of negative hydroxide ions ( $OH^-$ ) as a result of increasing the pH value, which led to rise the repulsive force between the adsorbent surface and the dye molecules (Alalwan et al., 2021).

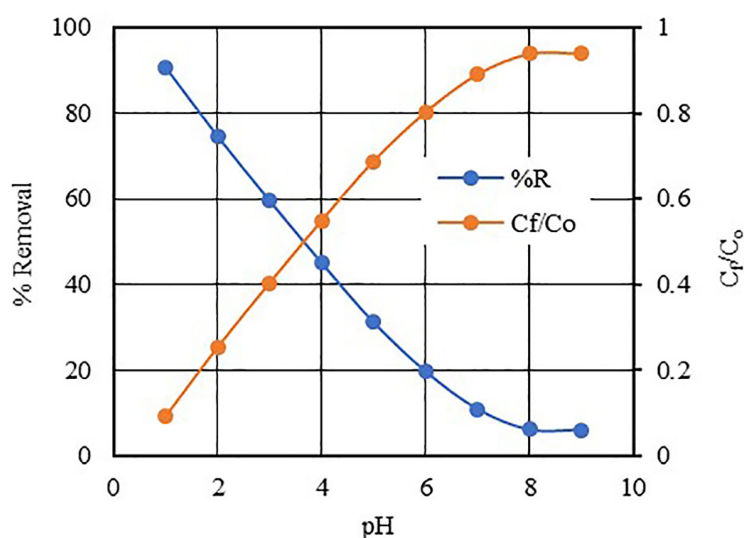
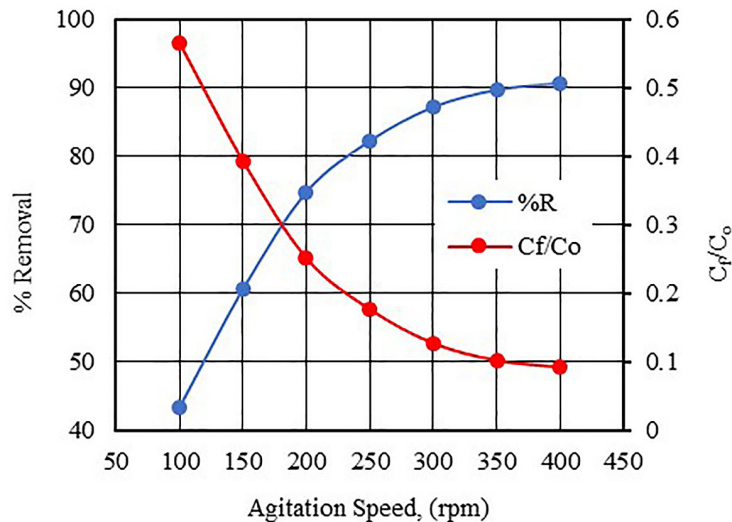


Figure 8. Effect of pH on the bromophenol blue dye removal



**Figure 9.** Effect of agitation speed on the bromophenol blue dye removal

Therefore, the optimal pH value for the adsorption of bromophenol dye is determined to be 1.

### Impact of agitating speed

The experimental findings regarding the effect of agitation speed on the adsorption process are presented in Figure 9. The agitation speed was varied within the range of 100–400 rpm while maintaining other operational factors at their optimum values. As observed from the figure, the adsorption efficiency increases along with agitation speed until it reaches a value of 350 rpm, after which it remains constant without further changes. The increase in adsorption efficiency at higher agitation speeds can be attributed to several factors. Firstly, the higher agitation speed promotes better contact between the silicon dioxide nanoparticles and the bromophenol blue dye, enhancing the chances of dye molecules reaching the active sites on the adsorbent surface and reducing their concentration in the solution. Secondly, the increased mass transfer rate resulting from higher agitation speeds allows the bromophenol blue dye to rapidly move towards the adsorbing surface due to the enhanced kinetic energy.

Notably, the adsorption efficiency increased by double when the agitation speed was multiplied by 3.5. Figure 9 also demonstrates that the maximum adsorption capacity is achieved at an agitation speed of 400 rpm, after which no further increase is observed. This can be explained by the saturation of the adsorption sites on the adsorbent material (Abbas and Ibrahim, 2020). At this point, the adsorbent has reached its maximum capacity

and is no longer capable of adsorbing additional dye molecules (Abdullah et al., 2023).

### Impact of initial concentration

Experimental trials were conducted to investigate the impact of varying the initial concentration of bromophenol blue dye while keeping other design parameters constant at their optimal values. The outcomes of this study are depicted in Figure 10, which illustrates the relationship between the initial concentration of bromophenol blue dye and both the adsorption efficiency and the adsorption concentration. As observed from the figure, there is a gradual decrease in the adsorption efficiency as the initial concentration of bromophenol blue dye increases. This can be attributed to the limited surface area and the fixed number of active sites available on the adsorbent material. Consequently, as the concentration of bromophenol blue dye increases, the number of available binding sites becomes insufficient to accommodate all the dye molecules, leading to a decrease in the adsorption efficiency. On the other hand, Figure 10 reveals an increase in the adsorbed concentration compared to the initial concentration. This is due to the calculation method, where the adsorbed concentration is obtained by subtracting the remaining concentration in the solution from the initial concentration. With an increase in the initial concentration, the adsorbed concentration also rises until it reaches a constant value. This constant value represents the maximum amount of bromophenol blue dye molecules that can be absorbed by the nanoparticles. The results indicate that the maximum adsorbent

concentration achieved is about  $170.4 \text{ mg}\cdot\text{g}^{-1}$ , obtained at an initial concentration of 120 ppm. This optimal initial concentration was utilized for the subsequent adsorption experiments. It is worth noting that similar findings have been reported in previous studies, such as (Abbas and Abbas, 2014) validating the consistency of the obtained results with the existing literature.

### Behavior of adsorbent dose

The impact of the adsorbent dosage, specifically the prepared silicon dioxide nanoparticles, on the efficiency of bromophenol blue dye

removal from aqueous solutions is demonstrated in Figure 11. The graph illustrates a direct relationship between the removal percentage and the quantity of silicon dioxide nanoparticles employed. Increasing the adsorbent amount leads to a higher removal percentage, indicating an enhanced treatment efficiency. By increasing the dosage of the adsorbent, the number of active sites available for adsorption increases. This is due to the constant surface area per unit mass of the adsorbent material. Consequently, an increased number of functional groups are available to interact with and adsorb bromophenol blue dye particles from the aqueous solution, resulting in improved treatment efficiency. It is

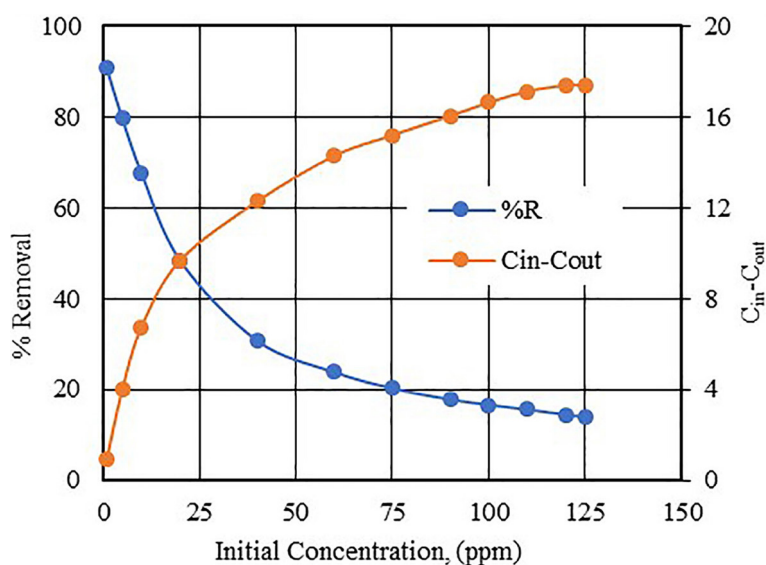


Figure 10. Effect of initial concentration on bromophenol blue dye removal

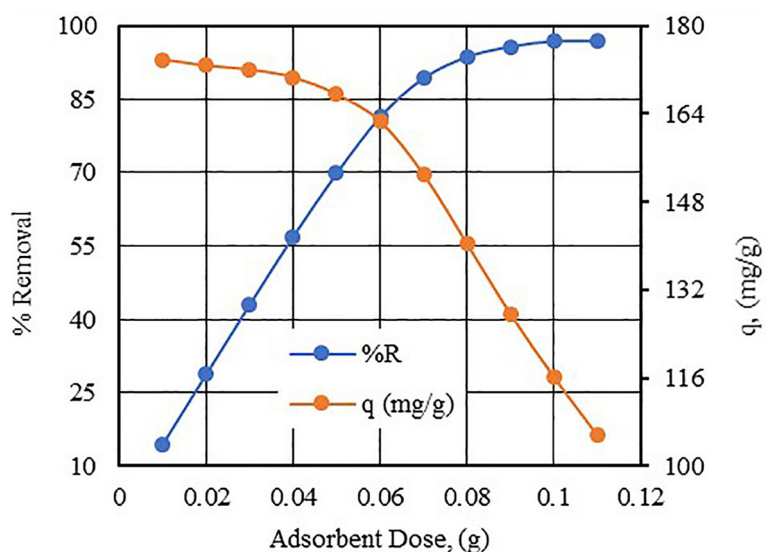


Figure 11. Effect of adsorbent dose on bromophenol blue dye removal

worth noting that Figure 11 also highlights the gradual increase in the removal efficiency, ranging from a minimum of 15% to a maximum of 96.851%, as the dosage increases from 0.01 g to 0.1 g, respectively. Beyond this point, the removal percentage reaches a plateau and remains constant. This can be attributed to the saturation of the active sites on the surface of the silicon dioxide nanoparticles, limiting further adsorption of dye molecules from the contaminated solution. On the basis of these findings, it can be concluded that an optimum dosage of 0.1 g of prepared silicon dioxide nanoparticles ensures the highest treatment efficiency for aqueous

solutions contaminated with bromophenol blue dye (Ibrahim et al., 2021).

### Behavior of contact time

The impact of contact time on the removal of bromophenol blue dye using silicon dioxide nanoparticles was investigated while keeping other variables at their optimum values. The contact time varied from 10 to 150 minutes. As depicted in Figure 12, the efficiency of bromophenol blue dye removal increases with prolonged contact time. The removal percentage starts at its lowest value and progressively rises to its peak of 96.851 at 2 hours. The extended

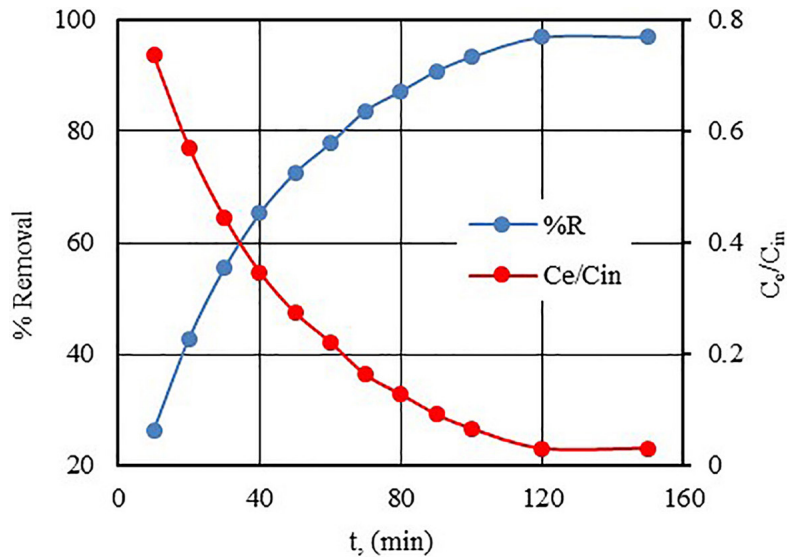


Figure 12. Effect of contact time on bromophenol blue dye removal

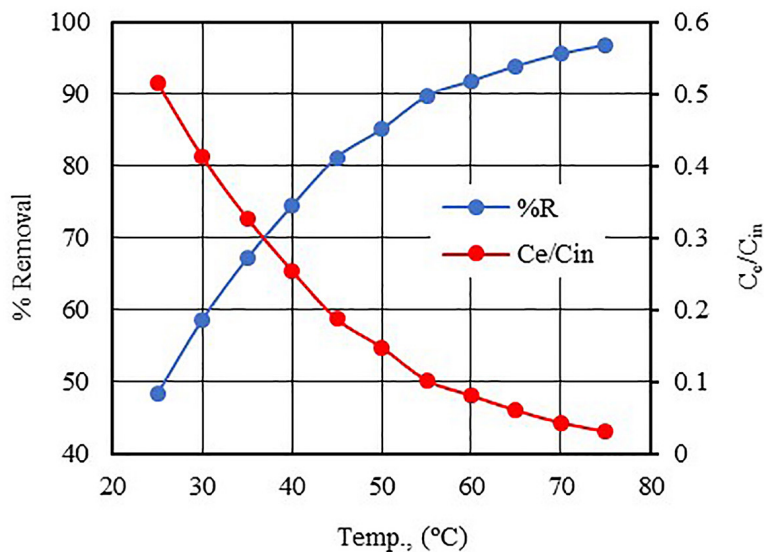


Figure 13. Effect of temperature on bromophenol blue dye removal

contact time enhances the adsorption of dye molecules at the active sites on the adsorbent surface, resulting in a decrease in dye concentration within the solution and consequently an increase in the removal percentage. Beyond the duration of 120 minutes, the removal efficiency reaches a steady state. This can be attributed to the saturation of active sites under the prevailing operational conditions (Abbas et. al., 2021). Therefore, a contact time of 2 hours is deemed optimal for achieving the highest removal efficiency of bromophenol blue dye from contaminated aqueous solutions.

### Impact of temperature

The impact of temperature on the adsorption capacity of bromophenol blue dye was investigated over a temperature range of 20–50 °C, encompassing the typical climatic conditions experienced in Iraq throughout the year. Figure 13 presents the results of the percentage removal efficiency obtained by varying the temperature in the adsorption process. It is evident from the figure that the efficiency of the adsorption process increases along with temperature, indicating a direct relationship between temperature and removal efficiency. Temperature plays a direct role in influencing the two key factors of the adsorption process: the adsorbate and the adsorbent surface. The current results indicate that temperature has a more pronounced effect on the adsorbent material compared to its impact on the adsorption surface. The increase in temperature enhances the kinetic energy of bromophenol blue dye, which increases its speed and thus the chance of it reaching the active sites on the surface of the adsorbent media (Mohammed et. al., 2022). In addition to that, raising the temperature may lead to an expansion of the adsorption surface pores, which would allow the absorption of a larger amount of bromophenol blue dye molecules and thus increase the efficiency of the treatment process, by increasing the susceptibility of the material to adsorb a further amount of dye from the contaminated solution. Figure 13 indicates that raising the temperature from 20 to 50 °C has improved the adsorption efficiency by approximately 50%. These results align with the observations reported in the study conducted by Ghulam et al., 2020.

## CONCLUSIONS

This study focused on the synthesis of silicon dioxide nanoparticles through a green method utilizing a buckthorn leaves extract and potassium metasilicate ( $K_2SiO_3$ ) as the precursor. Morphological examinations were conducted on the prepared nanoparticles, and the FTIR analysis revealed the presence of multiple functional groups, including Si-O-Si, Si-OH, and various alkyl groups. Additionally, FESEM testing demonstrated that the nanoparticles exhibited a spherical shape, interconnected with each other, and displayed a distinct porous surface structure. Furthermore, XRD analysis confirmed that the prepared nanoparticles were of pure single-phase, aligning perfectly with the reference JCPDS file No. 89–0510 for  $SiO_2$ . The BET test based on the adsorption-desorption of nitrogen indicated a measured surface area of  $246 \text{ m}^2 \cdot \text{g}^{-1}$  for the prepared nanoparticles, while the DSL test determined the particle size to be 135.8 nm. The  $SiO_2$  nanoparticles showcased a remarkable ability as an adsorbent media for effectively removing bromophenol blue dye from contaminated aqueous solutions across various operational parameters. The maximum adsorption efficiency per gram of nanoparticle surpassed 96% at initial concentrations of 120 ppm, a pH of 1, an agitation speed of 350 rpm, a contact time of 2 hours, and at laboratory temperature. Consequently, the prepared silicon dioxide nanoparticles proved to be highly active adsorbents, showcasing great potential in the treatment of polluted wastewater.

### Acknowledgement

The authors would like to thank Mustansiriyah University ([www.uomustansiriyah.edu.iq](http://www.uomustansiriyah.edu.iq)) Baghdad – Iraq for its support in the present work.

## REFERENCES

1. Abbas F.S., Abdulkareem W.S., Abbas M.N. 2022. Strength Development of Plain Concrete Slabs by the Sustainability Potential of Lead-Loaded Rice Husk (LLRH). *Journal of Applied Engineering Science*, 20(1), 160–167. <https://doi:10.5937/jaes0-32253>
2. Abbas M.N., Abbas F.S. 2013a. Iraqi Rice Husk Potency to Eliminate Toxic Metals from Aqueous Solutions and Utilization from Process Residues. *Advances in Environmental Biology*, 7(2), 308–319.
3. Abbas M.N., Abbas F.S. 2013b. The Predisposition

- of Iraqi Rice Husk to Remove Heavy Metals from Aqueous Solutions and Capitalized from Waste Residue. *Research Journal of Applied Sciences, Engineering and Technology*, 6(22), 4237–4246.
4. Abbas M.N., Abbas F.S. 2013c. The Feasibility of Rice Husk to Remove Minerals from Water by Adsorption and Avail from Wastes. *Research Journal of Applied Sciences, WSEAS Transactions on Environment and Development*, 9(4), 301–313.
  5. Abbas M.N., Abbas F.S. 2014. Application of Rice Husk to Remove Humic Acid from Aqueous Solutions and Profiting from Waste Leftover. *WSEAS Transactions on Biology and Biomedicine*, 11(9), 62–69.
  6. Abbas M.N., Alalwan H.A. 2019. Catalytic Oxidative and Adsorptive Desulfurization of Heavy Naphtha Fraction. *Korean Journal of Chemical Engineering*, 12(2), 283–288. <http://doi.org/10.9713/kcer.2019.57.2.283>
  7. Abbas M.N., Ibrahim S.A. 2020. Catalytic and thermal desulfurization of light naphtha fraction. *Journal of King Saud University - Engineering Sciences*, 32(4), 229–235. <https://doi.org/10.1016/j.jksues.2019.08.001>
  8. Abbas M.N., Nussrat T.H. 2020. Statistical Analysis of Experimental Data for Adsorption Process of Cadmium by Watermelon Rinds in Continuous Packed Bed Column. *International Journal of Innovation, Creativity and Change*, 13(3), 124–138.
  9. Abbas M.N., Ali S.T., Abbas R.S. 2020. Rice Husks as a Biosorbent Agent for Pb<sup>+2</sup> Ions from Contaminated Aqueous Solutions: A Review. *Biochemical and Cellular Archives*, 20(1), 1813–1820. <https://doi.org/10.35124/bca.2020.20.1.1813>
  10. Abbas M.N., Al-Madhhachi A.T., Esmael S.A. 2019a. Quantifying soil erodibility parameters due to wastewater chemicals. *International Journal of Hydrology Science and Technology*, 9(5), 550–568. <http://doi.org/10.1504/IJHST.2019.10016884>
  11. Abbas M.N., Al-Hermizy S.M.M., Abudi Z.N., Ibrahim T.A. 2019b. Phenol Biosorption from Polluted Aqueous Solutions by *Ulva lactuca* Alga using Batch Mode Unit. *Journal of Ecological Engineering*, 20(6), 225–235. <https://doi.org/10.12911/22998993/109460>
  12. Abbas M.N., Al-Tameemi I.M., Hasan M.B., Al-Madhhachi A.T. 2021. Chemical Removal of Cobalt and Lithium in Contaminated Soils using Promoted White Eggshells with Different Catalysts. *South African Journal of Chemical Engineering*, 35, 23–32. <https://doi.org/10.1016/j.sajce.2020.11.002>
  13. Abbas M.N., Ibrahim S.A., Abbas Z.N., Ibrahim T.A. 2022. Eggshells as a Sustainable Source for Acetone Production. *Journal of King Saud University - Engineering Sciences*, 34(6), 381–387. <https://doi.org/10.1016/j.jksues.2021.01.005>
  14. Abbas M.N. 2015. Phosphorus removal from wastewater using rice husk and subsequent utilization of the waste residue. *Desalination and Water Treatment*, 55(4), 970–977. <https://doi.org/10.1080/19443994.2014.922494>
  15. Abdulkareem W.S., Aljumaily H.S.M., Mushatat H.A., Abbas M.N. 2023. Management of Agro-Waste by Using as an Additive to Concrete and Its Role in Reducing Cost Production: Impact of Compressive Strength as a Case Study. *International Journal on Technical and Physical Problems of Engineering (IJTPE)*, 1(1), 62–67.
  16. Abdullah W.R., Alhamadani Y.A.J., Abass I.K., Abbas M.N. 2023. Study of chemical and physical parameters affected on purification of water from inorganic contaminants. *Periodicals of Engineering and Natural Sciences*, 11(2), 166–175. <http://dx.doi.org/10.21533/pen.v11i2.3508>
  17. Abd Ali I.K., Salman S.D., Ibrahim T.A., Abbas M.N., 2024. Study of the teratogenic effects of antimony on liver in the adult rabbit (*Oryctolagus cuniculus*). *Advancements in Life Sciences*, 11(2), 462–469.
  18. Al-Ali S.I.S., Abudi Z.N., Abbas M.N. 2023. Modelling and Simulation for the use of Natural Waste to Purified Contaminated Heavy Metals. *Journal of the Nigerian Society of Physical Sciences*, 5(1), 1143. <https://doi.org/10.46481/jnsps.2023.1143>
  19. Alalwan H.A., Abbas M.N., Alminshid A.H. 2020. Uptake of Cyanide Compounds from Aqueous Solutions by Lemon Peel with Utilising the Residue Absorbents as Rodenticide. *Indian Chemical Engineer*, 62(1), 40–51. <https://doi.org/10.1080/00194506.2019.1623091>
  20. Alalwan H.A., Abbas M.N., Abudi Z.N., Alminshid A.H. 2018. Adsorption of thallium ion (Tl<sup>+3</sup>) from aqueous solutions by rice husk in a fixed-bed column: Experiment and prediction of breakthrough curves. *Environmental Technology and Innovation*, 12, 1–13. <https://doi.org/10.1016/j.eti.2018.07.001>
  21. Alalwan H.A., Mohammed M.M., Sultan A.J., Abbas M.N., Ibrahim T.A., Aljaafari H.A.S., Alminshid A.A. 2021. Adsorption of methyl green stain from aqueous solutions using non-conventional adsorbent media: Isothermal kinetic and thermodynamic studies. *Bioresource Technology Reports*, 14, 100680. <https://doi.org/10.1016/j.biteb.2021.100680>
  22. Alalwan H.A., Alminshid A.H., Mohammed M.M., Hussein S.A.M., Mohammed M.F. 2022a. Employing Synthesized MgO-SiO<sub>2</sub> Nanoparticles as Catalysts in Ethanol Conversion to 1,3-Butadiene. *International Journal of Nanoscience*, 18(3), 157–166.
  23. Alalwan H.A., Alminshid A., Mohammed M.M., Mohammed M.F., Shadhar M.H. 2022b. Reviewing of using Nanomaterials for Wastewater Treatment. *Pollution*, 8(3), 995–1013. <https://doi.org/10.22059/>

- poll.2022.337436.1329
24. Alhamd S.J., Abbas M.N., Manteghian M., Ibrahim T.A., Jarmondi K.D.S. 2024a. Treatment of oil refinery wastewater polluted by heavy metal ions via adsorption technique using non-valuable media: cadmium ions and buckthorn leaves as a study case. *Karbala International Journal of Modern Science*, 10(1), 1–18. <https://doi.org/10.33640/2405-609X.3334>
  25. Alhamd S.J., Abbas M.N., Al-Fatlawy H.J.J., Ibrahim T.A., Abbas Z.N. 2024b. Removal of phenol from oilfield produced water using non-conventional adsorbent medium by an eco-friendly approach. *Karbala International Journal of Modern Science*, 10(2), 191-210. <https://doi.org/10.33640/2405-609X.3350>
  26. Al-Hermizy S.M.M., Al-Ali S.I.S., Abdulwahab I.A., Abbas M.N. 2022. Elimination of Zinc Ions ( $Zn^{+2}$ ) from Synthetic Wastewater Using Lemon Peels. *Asian Journal of Water, Environment and Pollution*, 19(5), 79–85. <https://doi.org/10.3233/AJW220073>
  27. Ali G.A.A., Abbas M.N. 2020. Atomic Spectroscopy Technique Employed to Detect the Heavy Metals from Iraqi Waterbodies Using Natural Bio-Filter (*Eichhornia crassipes*) Thera Dejlja as a Case Study. *Systematic Reviews in Pharmacy*, 11(9), 264–271. <https://doi.org/10.31838/srp.2020.9.43>
  28. Ali G.A.A., Ibrahim S.A., Abbas M.N. 2021. Catalytic Adsorptive of Nickel Metal from Iraqi Crude Oil using non-Conventional Catalysts. *Innovative Infrastructure Solutions*, 6(7), 1–9. <https://doi.org/10.1007/s41062-020-00368-x>
  29. Ali S.A.K., Almhana N.M., Hussein A.A., Abbas M.N. 2020a. Purification of Aqueous Solutions from Toxic Metals using Laboratory Batch Mode Adsorption Unit Antimony (V) Ions as a Case Study. *Journal of Green Engineering (JGE)*, 10(11), 10662–10680.
  30. Ali S.T., Qadir H.T., Moufak S.K., Al-Badri M.A.M., Abbas M.N. 2020. A Statistical Study to Determine the Factors of Vitamin D Deficiency in Men the City of Baghdad as a Model. *Indian Journal of Forensic Medicine & Toxicology*, 14(1), 691–696. <https://doi.org/10.37506/ijfnt.v14i1.132>
  31. Aljubiri S.M., El-Shwiniy W.H., Younes A.A.O., Alosaimi E.H., El-Wahaab B.A. 2023. Use of *Euphorbia balsamifera* Extract in Precursor Fabrication of Silver Nanoparticles for Efficient Removal of Bromocresol Green and Bromophenol Blue Toxic Dyes. *Molecules (Basel, Switzerland)*, 28(9), 3934. <https://doi.org/10.3390/molecules28093934>
  32. Alminshid A.H., Abbas M.N., Alalwan H.A., Sultan A.J., Kadhome M.A. 2021. Aldol condensation reaction of acetone on MgO nanoparticles surface: An *in-situ* drift investigation. *Molecular Catalysis*, 501, 111333. <https://doi.org/10.1016/j.mcat.2020.111333>
  33. Alshoaibi A., Islam S. 2021. Synthesis and characterization of bromophenol blue encapsulated silica and silica-titania nanocomposites for detection of volatile organic vapors. *Physica B: Condensed Matter*, 614, 413026. <https://doi.org/10.1016/j.physb.2021.413026>
  34. Alwan E.K., Hammoudi A.M., Abd I.K., Abd Alaa M.O., Abbas M.N. 2021. Synthesis of Cobalt Iron Oxide Doped by Chromium Using Sol-Gel Method and Application to Remove Malachite Green Dye. *NeuroQuantology*, 19(8), 32–41. <http://doi:10.14704/nq.2021.19.8.NQ21110>
  35. Batubara A.S., Ainousah B.E., Gamal M., Almrasy A.A., Ramzy S., Ghoneim M.M., Abdelazim A.H. 2023. Green-adapted spectrophotometric determination of fostemsavir based on selective bromophenol blue extraction; reduction of hazardous consumption using computational calculations. *Scientific reports*, 13(1), 10049. <https://doi.org/10.1038/s41598-023-36821-x>
  36. Ghulam N.A., Abbas M.N., Sachit D.E. 2020. Preparation of synthetic alumina from aluminium foil waste and investigation of its performance in the removal of RG-19 dye from its aqueous solution. *Indian Chemical Engineer*, 62(3), 301–313. <https://doi.org/10.1080/00194506.2019.1677512>
  37. Hamdi G.M., Abbas M.N., Ali S.A.K. 2024. Bioethanol Production from Agricultural Waste: A Review. *Journal of Engineering and Sustainable Development*, 28(2), 233–252. <https://doi.org/10.31272/jeasd.28.2.7>
  38. Hanafi M.F., Sapawe N. 2020. A review on the water problem associate with organic pollutants derived from phenol, methyl orange, and remazol brilliant blue dyes. *Materials Today: Proceedings*, 31, A141–A150. <https://doi.org/10.1016/j.matpr.2021.01.258>
  39. Hasan M.B., Al-Tameemi I.M., Abbas M.N. 2021. Orange Peels as a Sustainable Material for Treating Water Polluted with Antimony. *Journal of Ecological Engineering*, 22(2), 25–35. <https://doi.org/10.12911/22998993/130632>
  40. Hashem N.S., Ali G.A.A., Jameel H.T., Khurshid A.N., Abbas M.N. 2021. Heavy Metals Evaluation by Atomic Spectroscopy, for Different Parts of Water Hyacinth (*Eichhornia crassipes*) Plants Banks of Tigris River. *Biochemical and Cellular Archives*, 21(2), 3813–3819. <https://connectjournals.com/03896.2021.21.3813>
  41. Hassen J., Ayfan A., Joudah M. 2022. Determination of the Optimal Adsorbent for Bromophenol Blue Dye: Adsorption from Aqueous Solution. *Egyptian Journal of Chemistry*, 65, 131, 645–651. <https://doi.org/10.21608/ejchem.2022.128570.5692>
  42. Ho, S. 2022. Low-Cost Adsorbents for the Removal of Phenol/Phenolics, Pesticides, and Dyes from Wastewater Systems: A Review. *Water*, 14(20), 3203. <https://doi.org/10.3390/w14203203>

43. Ibrahim S.A., Hasan M.B., Al-Tameemi I.M., Ibrahim T.A., Abbas M.N. 2021. Optimization of adsorption unit parameter of hardness remediation from wastewater using low-cost media. *Innovative Infrastructure Solutions*, 6(4), Article number: 200. <https://doi.org/10.1007/s41062-021-00564-3>
44. Ibrahim T.A., Mahdi H.S., Abbas R.S., Abbas, M.N. 2020b. Study the effect of ribavirin drug on the histological structure of the testes in Albino mice (*Mus musculus*). *Journal of Global Pharma Technology*, 12,(2), 142–146.
45. Ibrahim T.A., Mohammed A.M., Abd ali I.K., Abbas M.N., Hussien S.A. 2020a. Teratogenic Effect of Carbamazepine Drug on the Histological Structure of Testes in the Albino Mouse (*Mus musculus*). *Indian Journal of Forensic Medicine & Toxicology*, 14(4), 1829–1834. <https://doi.org/10.37506/ijfmt.v14i4.11809>
46. Khaleel L.R., Al-Hermizy, S. M., Abbas, M.N. 2022. Statistical indicators for evaluating the effect of heavy metals on samaraa drug industry water exposed to the sun and freezing. *Tropical Journal of Natural Product Research*, 6(12), 1969–1974. <http://www.doi.org/10.26538/tjnpr/v6i12.12>
47. Kolya H., Kang C.-W. 2024. Toxicity of metal oxides, dyes, and dissolved organic matter in water: implications for the environment and human health. *Toxics*, 12(2), 111. <https://doi.org/10.3390/toxics12020111>
48. Maddodi S.A., Alalwan H.A., Alminshid A.H., Abbas M.N. 2020. Isotherm and computational fluid dynamics analysis of nickel ion adsorption from aqueous solution using activated carbon. *South African Journal of Chemical Engineering*, 32, 5–12. <https://doi.org/10.1016/j.sajce.2020.01.002>
49. Mohammed Ali N.S., Alalwan H.A., Alminshid A.H., Mohammed M.M. 2022. Synthesis and Characterization of Fe<sub>3</sub>O<sub>4</sub>-SiO<sub>2</sub> Nanoparticles as Adsorbent Material for Methyl Blue Dye Removal from Aqueous Solutions. *Pollution*, 8(1), 295–302. <http://doi.org/10.22059/poll.2021.328697.1157>
50. Mohammed M.M., Alalwan H.A., Alminshid A., Hussein S.A.M., Mohammed M.F. 2022. Desulfurization of heavy naphtha by oxidation-adsorption process using iron-promoted activated carbon and Cu<sup>+2</sup>-promoted zeolite 13X. *Catalysis Communications*, 169, 106473. <https://doi.org/10.1016/j.catcom.2022.106473>
51. National Center for Biotechnology Information (NCBI). 2023. PubChem Compound Summary for CID 8272, Bromophenol Blue. Retrieved August 9, from <https://pubchem.ncbi.nlm.nih.gov/compound/Bromophenol-Blue>
52. Rajaa N., Kadhim F.J., Abbas M.N., Banyhussan Q.S. 2023, The improvement of concrete strength through the addition of sustainable materials (agro-waste loaded with copper ions). 3<sup>rd</sup> International Conference for Civil Engineering Science (ICCES 2023), IOP Conf. Series: Earth and Environmental Science, 1232, 012038, 9. <http://doi.org/10.1088/1755-1315/1232/1/012038>
53. Srivatsav P., Bhargav B.S., Shanmugasundaram V., Arun J., Gopinath K.P., Bhatnagar A. 2020. Biochar as an eco-friendly and economical adsorbent for the removal of colorants (dyes) from aqueous environment: A review. *Water*, 12(12), 3561. <https://doi.org/10.3390/w12123561>
54. Tolkou A.K., Tsoutsas E.K., Kyzas G.Z., Katsoyianis I.A. 2024. Sustainable use of low-cost adsorbents prepared from waste fruit peels for the removal of selected reactive and basic dyes found in wastewaters. *Environmental Science and Pollution Research*. <https://doi.org/10.1007/s11356-024-31868-3>
55. Williams T.N., Vacchi F.I., dos Santos A., Aragão Umbuzeiro G. de, Freeman H.S. 2022. Metal-complexed monoazo dyes as sustainable permanent hair dye alternatives – toxicological and durability properties. *Dyes and Pigments*, 197, 109819. <https://doi.org/10.1016/j.dyepig.2021.109819>